Chinese Chemical Letters 34 (2023) 107676

Contents lists available at ScienceDirect

Chinese Chemical Letters

journal homepage: www.elsevier.com/locate/cclet

Employing halogen-halogen interaction to construct high-temperature hybrid perovskite phase transition materials

Dongying Fu[a,b,*], Zuoming Hou[a], Zhuo Chen[a], Yueyue He[a], Xian-Ming Zhang[a]

[a] Institute of Crystalline Materials, Shanxi University, Taiyuan 030006, China
[b] State Key Laboratory of Quantum Optics and Quantum Optics Devices, Shanxi University, Taiyuan 030006, China

ARTICLE INFO

Article history:
Received 30 May 2022
Revised 8 June 2022
Accepted 12 July 2022
Available online 14 July 2022

Keywords:
Halogen-halogen interaction
Phase transition
Hybrid perovskite
Molecular designing

ABSTRACT

Organic-inorganic hybrid perovskites (OIHPs) materials with high phase transition temperature (T_p) have been widely studied in the field of molecular switches, solar energy and electric power. At present, the OIHPs with high T_p are generally constructed through molecular design, which can be applied to a wide temperature range. Here, three one-dimensional (1D) OIHPs [*R*-ClEQ]$PbCl_3$ ($T_p = 442$ K), [*R*-ClEQ]$PbBr_3$ ($T_p = 499$ K) and [*R*-ClEQ]PbI_3 (T_p above m.p.) (*R*-ClEQ = (*R*)-*N*-chloroethyl-3-quinuclidinol) with different T_p are obtained by regulating the halogen-halogen interaction and hydrogen bonding in the system. Especially in [*R*-ClEQ]PbX_3 (X = Cl, Br and I) crystal system, all the halogen bonds tend to form at approximately 180°angles and the strength of halogen bonding is found to be increased from 1.59×10^{-3} Hartree to 2.35×10^{-3} Hartree with increased atom number from Cl to I. The synergistic effect of halogen bonding and hydrogen bonding provide a useful strategy for the design OIHPs phase transition materials with high T_p.

Organic-inorganic hybrid perovskites (OIHPs) phase transition materials (PTMs) have a wide range of applications in data storge, solar cell, molecular switches and so on [1–6]. Due to the advantages of structural adjustability, good film-forming and variety, which make it become a useful supplement to the traditional inorganic PTMs [7–9]. As an important index, the phase transition temperature (T_p) of OIHPs determines the application temperature range of materials. Compared with inorganic perovskite $BaTiO_3$ ($T_p = 393$ K) [10], OIHPs combine the merits of inorganic and organic components, which makes it possible to accurately construct high-temperature PTMs through molecular tailoring tactics [11]. For example, Xiong *et al.* propose to design high-temperature multifunctional PTMs through H/F substitute strategy, and a series of OIHPs with excellent properties emerge in endlessly, such as $[PFBA]_2PbBr_4$ (PFBA) (PFBA = perfluorobenzylammonium) ($T_p = 440$ K), $[2\text{-FBA}]_2PbCl_4$ (2-FBA = 2-fluorobenzylammonium) ($T_p = 448$ K), $[4,4\text{-DFHHA}]_2PbI_4$ (4,4-DFHHA = 4,4-difluorohexahydroazepine) ($T_p = 454$ K), [*N*-FMedabco]PbI_3 (*N*-FMedabco = *N*-fluoromethyldabconium) ($T_p = 473$ K) [12]. Surprisingly, the T_p of these fluorinated compounds is higher than that of prototype. This strategy is mainly due to the stronger electronegativity of F atoms and the stronger hydrogen bond in the system after F substitution. In addition, F atom is heavier than H atom, which increases the energy barrier to be overcome in the process of phase transition. Similarly, the deuterium isotope effect is always recognized as an effective tool for enhancing the T_p, but it can only be applied to the limited system [13,14].

Because of the characteristics of inorganic and organic components, there are many intermolecular interactions in the OIHPs systems, such as hydrogen bonding, halogen-halogen bonding and Van der Waals forces between the ammonium cations [15,16]. Recent studies have shown that enhancing the intermolecular interaction is beneficial to rise the T_p of materials. For example, starting from proto counterpart $(C_4H_{10}N)[CdCl_3]$ ($T_p = 240$ K), a high temperature PTM (*R*/*S*)−3-OH-$(C_4H_9N)[CdCl_3]$ ($T_p = 350$ K) is synthesized by introducing hydroxyl functional groups through molecular tailoring [16]. Another compound is [DMEA]$PbBr_3$ (DMEA = *N*,*N*-dimethylethanolammonium), which also exhibits a high T_p at around 444 K [15]. These are mainly due to the introduction of hydroxyl enhances the intermolecular hydrogen bonding interactions. It seems commonly to regulate the T_p of the systems by hydrogen bonding, however, employing halogen-halogen interaction to construct high-temperature OIHPs PTMs is rarely reported. At present, there are mainly the following studies on the influence between halogen bonding and the properties of

* Corresponding author at: Institute of Crystalline Materials, Shanxi University, Taiyuan 030006, China.
E-mail address: dyfu@sxu.edu.cn (D. Fu).

https://doi.org/10.1016/j.cclet.2022.07.019
1001-8417/

materials. For example, Yuan *et al.* have reported the halogen-halogen bonds enable improved long-term operational stability of mixed-halide perovskite photovoltaics [17], Li *et al.* have studied the halogen bond passivated lead iodide perovskite surface through the first-principles calculations [18], Gratzel group [19], Loo group [20] and Snaith *et al.* [21] have proved the supramolecular halogen bond can passivation of OIHPs solar cells and enhance the stability. In addition to improve the stability of the OIHPs based device, employing the halo-functional design strategy is beneficial to charge mobilities in charge-transport layers and improve the solar energy conversion of devices [22–24]. These mentioned above are enough to prove that as an intermolecular interaction, halogen-halogen interaction can regulate the properties of materials. However, the research on regulating the T_p of the system through halogen bonding is still in its infancy.

Base on this, we employing the halogen-halogen interaction and hydrogen bonding to construct three one-dimensional (1D) OIHPs PTMs [*R*-ClEQ]$PbCl_3$ ($T_p = 442$ K), [*R*-ClEQ]$PbBr_3$ ($T_p = 499$ K) and [*R*-ClEQ]PbI_3 (T_p= above m.p.) (*R*-ClEQ = (*R*)-*N*-chloroethyl-3-quinuclidinol). In [*R*-ClEQ]PbX_3 (X = Cl, Br and I) system, with the increase of the atomic number of halogen (from Cl to I) on the inorganic chains, the interaction between halogen on the organic amine and halogen on the inorganic chains enhanced from 1.59×10^{-3} Hartree to 2.35×10^{-3} Hartree. Therefore, the combination of halogen-halogen interaction and hydrogen bonding provides a new strategy for regulating the T_p of PTMs.

Firstly, the crystals of [*R*-ClEQ]$PbCl_3$, [*R*-ClEQ]$PbBr_3$ and [*R*-ClEQ]PbI_3 are obtained through slow evaporation method in the HX (X = Cl, Br and I) solution containing organic amines and Pb salts (Scheme 1). The detailed preparation process is shown in the experimental section. Powder X-ray diffraction (PXRD) is used to confirm the phase purity, the PXRD diagrams of these compounds are shown in Figs. S1a-c (Supporting information). As we know that, the structure of the materials can affect the properties. In order to fundamentally analyze the structure differences of the three compounds, we carry out single crystal X-ray diffraction (SC-XRD) at room temperature in Fig. 1. It can be seen from Figs. 1a-c, the [*R*-ClEQ]$PbCl_3$, [*R*-ClEQ]$PbBr_3$ and [*R*-ClEQ]PbI_3 all adopt 1D chain structure. The difference is that in compound [*R*-ClEQ]$PbCl_3$ and [*R*-ClEQ]$PbBr_3$, the oxygen atom on the organic amine participates in the coordination with the central metal atom Pb, while in [*R*-ClEQ]PbI_3, the metal Pb is directly coordinated with six I atoms.

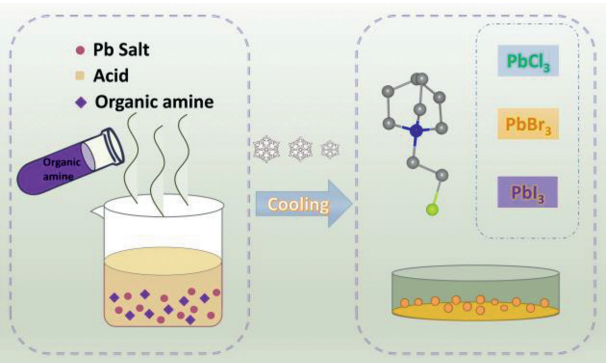

Scheme 1. The design of OIHPs phase transition materials.

Due to the change of coordination environment, the octahedrons in [*R*-ClEQ]$PbCl_3$ and [*R*-ClEQ]$PbBr_3$ tend to be connected in an edge-sharing manner to form 1D chain, while the octahedrons in [*R*-ClEQ]PbI_3 are connected in a face-sharing manner. Similar coordination patterns have also appeared in previously reported compounds [(*R*)-*N*-ethyl-3-quinuclidinol]$PbBr_3$ and [(*R*)-*N*-fluoroethyl-3-quinuclidinol]$PbBr_3$ [13]. The difference in structure leads to the crystallization of the three compounds in different space group. At room temperature, the [*R*-ClEQ]$PbCl_3$ and [*R*-ClEQ]$PbBr_3$ crystals crystallize in monoclinic $P2_1$ (point group:2) space group with cell parameters of $a = 9.1959(9)$ Å, $b = 9.2204(7)$ Å, $c = 9.5787(12)$ Å and $a = 9.4264(8)$ Å, $b = 9.4446(5)$ Å, $c = 9.7888(8)$ Å, respectively. The [*R*-ClEQ]PbI_3 adopt the orthorhombic space group $P2_12_12_1$ (point group: 222) with cell parameters of $a = 8.2758(8)$ Å, $b = 9.9484(8)$ Å and $c = 21.476(3)$ Å. Other crystal structure information, such as bond length and bond angle, are shown in Tables S1-S9 (Supporting information). Moreover, due to the involvement of oxygen atoms in coordination, the distortion degree of octahedron in these compounds is also different. Fig. 2 shows the bond lengths information of Pb-X (X = Cl, Br and I) and Pb-O bond in octahedrons. The bond length quadratic elongation (<λ>) is obtained through VESTA software, which shows that the larger the value of ⟨λ⟩, the more the octahedron is stretched. [25] The average ⟨λ⟩ of overall structure based on [*R*-ClEQ]$PbCl_3$, [*R*-ClEQ]$PbBr_3$ and [*R*-ClEQ]PbI_3 is calculated to be 1.0526, 1.0436 and 1.0132, respectively. Further-

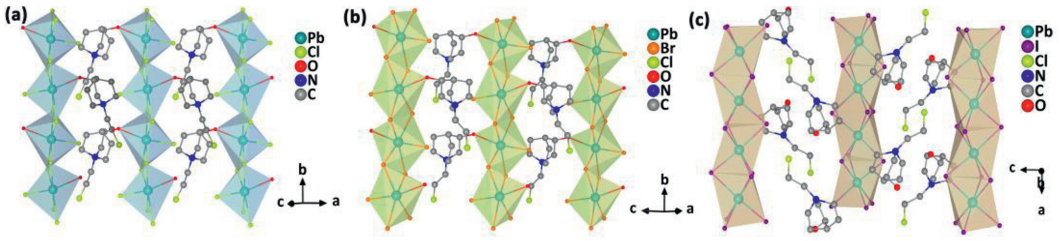

Fig. 1. Crystal structure of (a) [*R*-ClEQ]$PbCl_3$, (b) [*R*-ClEQ]$PbBr_3$ and (c) [*R*-ClEQ]PbI_3 at room temperature.

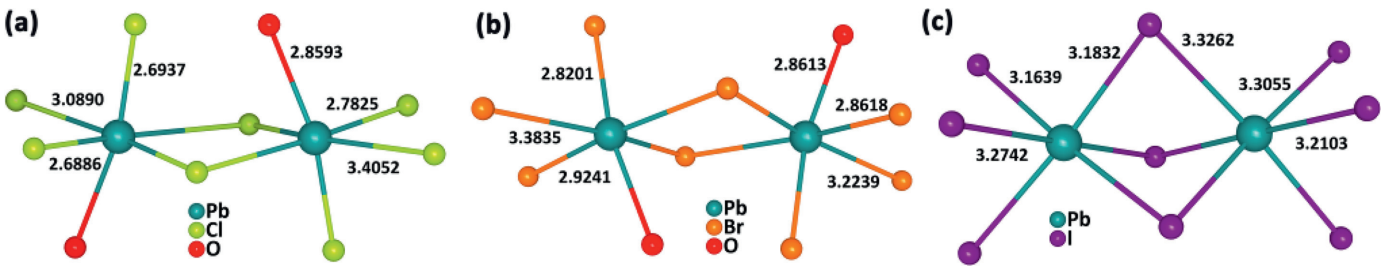

Fig. 2. The bond length of octahedrons in (a) [*R*-ClEQ]$PbCl_3$, (b) [*R*-ClEQ]$PbBr_3$ and (c) [*R*-ClEQ]PbI_3 (the unit is Å).

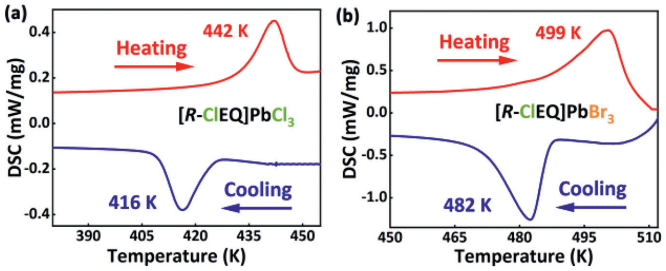

Fig. 3. DSC curves of (a)[*R*-ClEQ]$PbCl_3$ and (b) [*R*-ClEQ]$PbBr_3$.

more, the distortion degree of octahedron can be calculated according to the following formula:

$$\Delta d = 1/6\Sigma[(d_n - d)/d]^2 \quad (1)$$

where, d_n is the individual Pb-X (X = Cl, Br, I and O) bond length and d is the average Pb-X bond length [26,27]. The Δd is 6.77×10^{-3} for [*R*-ClEQ]$PbCl_3$, 4.58×10^{-3} for [*R*-ClEQ]$PbBr_3$ and 3.60×10^{-4} for [*R*-ClEQ]PbI_3. The results show that the octahedron in [*R*-ClEQ]$PbCl_3$ is highly distorted, which is consistent with the bond length quadratic elongation. Previous studies have shown that the distortion degree of octahedral in the system directly affects the luminescence and photoelectric properties of the materials [25,28,29]. The main reason for the difference of octahedral distortion is the significant different intermolecular interaction in the crystal. This also shows that the physical properties of the OIHPs can be regulated by intermolecular interaction.

Next, we study the phase transition of these three compounds in Fig. 3. The differential scanning calorimetry (DSC) of [*R*-ClEQ]$PbCl_3$, [*R*-ClEQ]$PbBr_3$ and [*R*-ClEQ]PbI_3 is executed under nitrogen atmosphere. The results indicate that a pair of distinct thermal anomalous peaks are observed at 442 K and 416 K for [*R*-ClEQ]$PbCl_3$ under heating and cooling process, respectively. Compared with [*R*-ClEQ]$PbCl_3$, the T_p of [*R*-ClEQ]$PbBr_3$ increased significantly, showing two peaks at 499 K and 482 K on the DSC curve. Unfortunately, no phase transition is found in [*R*-ClEQ]PbI_3 when it is heated to the melting point (m.p.), which may be caused by the T_p of [*R*-ClEQ]PbI_3 above the m.p. Moreover, the thermal hysteresis of [*R*-ClEQ]$PbCl_3$ and [*R*-ClEQ]$PbBr_3$ is 26 K and 17 K, respectively, which determine that the two compounds undergo a first-order phase transition process. In addition, the T_p of this series of compounds is generally higher than that of others, such as $(BA)_2PbCl_4$ (BA is benzylammonium, T_p is 438 K) [30], $EA_4Pb_3Cl_{10}$ (EA is ethylammonium, T_p is 415 K) [31], (DMAA)$CdCl_3$ (DMAA is *N*,*N*-dimethylallylammonium, T_p is 339 K) [32], $EA_4Pb_3Br_{10}$ (T_p is 384 K) [33].

In order to deeply study the reasons for the difference of T_p in these compounds, we analyze the intermolecular interactions in the system as follows, which generally play a critical role for determining and developing desired physical properties. As an effective characterization method, Hirshfeld surfaces and two-dimensional (2D) fingerprint plots are usually used to measure the intermolecular interactions, which is generated based on CIF files with structure factors through CrystalExplorer program [7,14,34]. For the Hirshfeld surfaces, the interactions in [*R*-ClEQ]PbI_3 (0.901, 0.700) is stronger than [*R*-ClEQ]$PbCl_3$ (0.991, 0.800) and [*R*-ClEQ]$PbBr_3$ (0.987, 0.795), which can also be directly seen from the minimum (d_i, d_e) in the 2D fingerprint plots in Figs. 4a-c. In addition, in the three systems, the hydrogen bonding formed with Cl on the organic amine is also different. The proportion of Cl···H interaction comprises 79.5%, 82.4% and 82.5% of the total Hirshfeld surface in [*R*-ClEQ]$PbCl_3$, [*R*-ClEQ]$PbBr_3$ and [*R*-ClEQ]PbI_3, respectively. This result shows that the hydrogen bonding in [*R*-ClEQ]PbI_3 is the strongest, followed by [*R*-ClEQ]$PbBr_3$, and the hydrogen bonding in [*R*-ClEQ]$PbCl_3$ is weakest. Therefore, it can also be seen that the

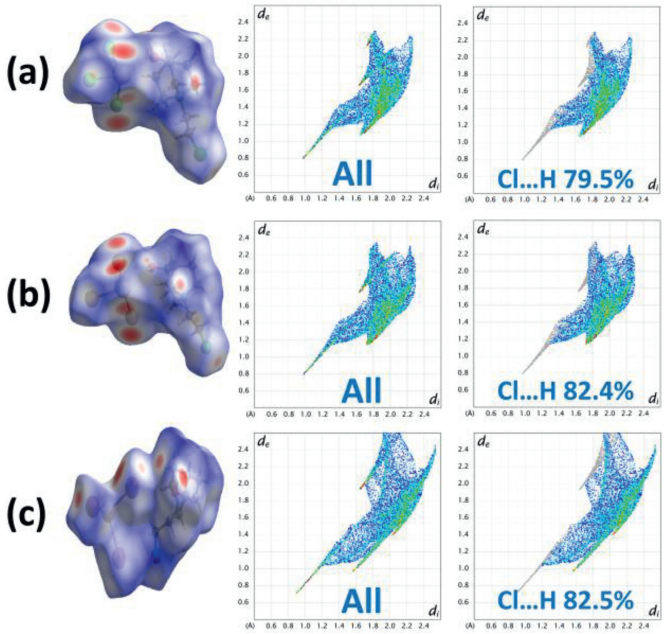

Fig. 4. Hirshfeld surface and related 2D fingerprint plot of (a) [*R*-ClEQ]$PbCl_3$, (b) [*R*-ClEQ]$PbBr_3$ and (c) [*R*-ClEQ]PbI_3.

strength of the hydrogen bonding in the system has a direct impact on the T_p.

Besides considering the hydrogen bonding, the interaction between halogen and halogen should not be ignored. Halogen bonding effect is being exploited for an important element in crystal engineering, which involves the utilization of the intermolecular interactions for the development of new molecular crystals with desired physical properties [22,35]. A halogen bond occurs when there is evidence of a net attractive interaction between an electrophilic region associated with a halogen atom in a molecular entity and a nucleophilic region in another, or the same, molecular entity. Due to the unique chemical nature of halogen bonding, this intermolecular interaction serves as an indispensable tool for the development of OIHPs crystal systems. In the [*R*-ClEQ]PbX_3 (X = Cl, Br and I) crystal system, all the halogen bonds tend to form at approximately 180° angles. The strength of halogen bonding is found to be increased from 1.59×10^{-3} Hartree to 2.35×10^{-3} Hartree with increased atom number (Fig. 5). The trend of energy enhancement is consistent with the increase of phase transition points for the three compounds. Therefore, the increased phase transition point may be attributed to a tighter combination of organic and inorganic moieties through directional halogen-halogen bonding.

In summary, three kinds of OIHPs PTMs [*R*-ClEQ]$PbCl_3$, [*R*-ClEQ]$PbBr_3$ and [*R*-ClEQ]PbI_3 are successfully synthesized. The T_p

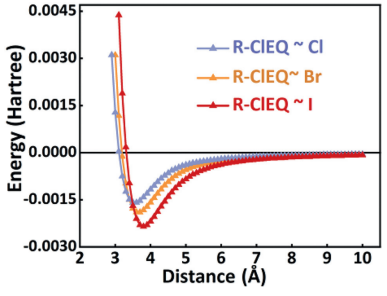

Fig. 5. The calculated halogen bond energy in the system of [*R*-ClEQ]PbX_3 (X = Cl, Br and I).

of the systems is accurately regulated by changing the intermolecular interactions in the crystal. The different intermolecular interactions lead to significant difference in the crystal structures of the three target compounds. Finally, due to the strong interaction of Cl-I bond, the T_p of [*R*-ClEQ]PbI_3 is above the m.p. In [*R*-ClEQ]$PbCl_3$ (442 K) and [*R*-ClEQ]$PbBr_3$ (499 K), the T_p increases with the enhancement of the interaction between Cl-Cl bond and Cl-Br bond. This work provides a useful supplement for the design of high-temperature PTMs by using intermolecular interactions, especially halogen-halogen interaction.

Declaration of competing interest

The authors declare no competing financial interest.

Acknowledgments

This work was financially supported by the National Natural Science Foundation of China (No. 22005183), the Program of State Key Laboratory of Quantum Optics and Quantum Optics Devices (No. KF202204) and the 1331 Project for Featured Chemistry Discipline in Shanxi Normal University.

Supplementary materials

Supplementary material associated with this article can be found, in the online version, at doi:10.1016/j.cclet.2022.07.019.

References

[1] W.Q. Liao, D.W. Zhao, Y.Y. Tang, et al., Science 363 (2019) 1206–1210.
[2] D.G. Billing, A. Lemmerer, New J. Chem. 32 (2008) 1736–1746.
[3] Y.Z. Hu, H.B. Zhang, W.K. Chong, et al., J. Phys. Chem. A 122 (2018) 6416–6423.
[4] M.M. Czka, A. Nowok, J.K. Zareba, et al., ACS Appl. Mater. Interfaces 14 (2022) 1460–1471.
[5] Y. Zeng, C.L. Hu, W.J. Xu, et al., Angew. Chem. Int. Ed. 61 (2022) e202110082.
[6] Q. Hu, H. Yu, S. Gong, et al., J. Mater. Chem. C 10 (2022) 6002–6008.
[7] S. Liu, L. He, Y. Wang, et al., Chin. Chem. Lett. 33 (2022) 1032–1036.
[8] X.G. Chen, Z.X. Zhang, Y.L. Zeng, et al., Chem. Commun. 58 (2022) 3059–3062.
[9] A. Lemmerer, Inorg. Chem. 61 (2022) 6353–6366.
[10] M.B. Smith, K. Page, T. Siegrist, et al., J. Am. Chem. Soc. 130 (2008) 6955–6963.
[11] H.Y. Liu, H.Y. Zhang, X.G. Chen, et al., J. Am. Chem. Soc. 142 (2020) 15205–15218.
[12] Y. Ai, H.P. Lv, Z.X. Wang, et al., Trends Chem. 3 (2021) 1088–1099.
[13] Y. He, Z. Chen, X. Chen, Mater. Chem. Front. 6 (2022) 1292–1300.
[14] L.L. Chu, T. Zhang, Y.F. Gao, et al., Chem. Mater. 32 (2020) 6968–6974.
[15] X.Q. Huang, H. Zhang, F. Wang, et al., J. Phys. Chem. Lett. 12 (2021) 5221–5227.
[16] H. Ye, W.H. Hu, W.J. Xu, et al., APL Mater. 9 (2021) 031102.
[17] X. Fu, T. He, S. Zhang, et al., Chem 7 (2021) 3131–3143.
[18] L. Zhang, X. Liu, J. Su, et al., J. Phys. Chem. C 120 (2016) 23536–23541.
[19] M.A. Ruiz-Preciado, D.J. Kubicki, A. Hofstetter, et al., J. Am. Chem. Soc. 142 (2020) 1645–1654.
[20] M.L. Ball, J.V. Milić, Y.L. Loo, Chem. Mater. 34 (2022) 2495–2502.
[21] A. Abate, M. Saliba, D.J. Hollman, et al., Nano Lett. 14 (2014) 3247–3254.
[22] P. Metrangolo, L. Canil, A. Abate, et al., Angew. Chem. Int. Ed. 61 (2022) e202114793.
[23] S. Bi, H. Wang, J. Zhou, et al., J. Mater. Chem. A 7 (2019) 6840–6848.
[24] L. Canil, J. Salunke, Q. Wang, et al., Adv. Energy Mater. 11 (2021) 2101553.
[25] Y. Fu, X. Jiang, X. Li, et al., J. Am. Chem. Soc. 142 (2020) 4008–4021.
[26] L. Mao, Y. Wu, C.C. Stoumpos, et al., J. Am. Chem. Soc. 139 (2017) 5210–5215.
[27] Y. Peng, Y. Yao, L. Li, et al., J. Mater. Chem. C 6 (2018) 6033–6037.
[28] D. Fu, S. Wu, Y. Liu, et al., Inorg. Chem. Front. 8 (2021) 3576–3580.
[29] B. Febriansyah, T. Borzda, D. Cortecchia, et al., Angew. Chem. Int. Ed. 59 (2020) 10791–10796.
[30] W.Q. Liao, Y. Zhang, C.L. Hu, et al., Nat. Commun. 6 (2015) 7338.
[31] S. Wang, L. Li, W. Weng, et al., J. Am. Chem. Soc. 142 (2020) 55–59.
[32] Z.X. Wang, H. Zhang, F. Wang, et al., J. Am. Chem. Soc. 142 (2020) 12857–12864.
[33] S. Wang, X. Liu, L. Li, et al., J. Am. Chem. Soc. 141 (2019) 7693–7697.
[34] H.Y. Zhang, Z.X. Zhang, X.J. Song, et al., J. Am. Chem. Soc. 142 (2020) 20208–20215.
[35] X.N. Hua, W.Q. Liao, Y.Y. Tang, et al., J. Am. Chem. Soc. 140 (2018) 12296–12302.